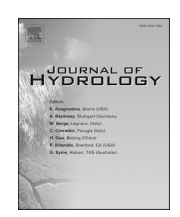
ELSEVIER

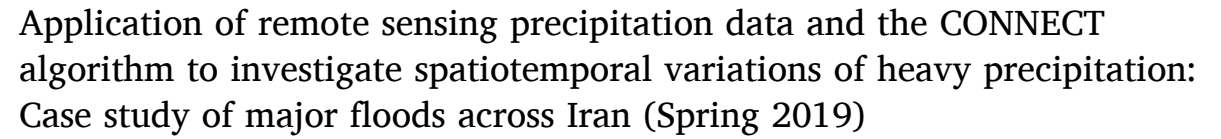
Contents lists available at ScienceDirect

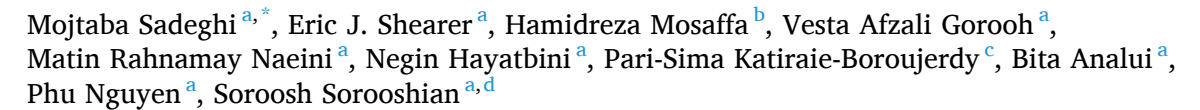
Journal of Hydrology

journal homepage: www.elsevier.com/locate/jhydrol



Research papers





- ^a Center for Hydrometeorology and Remote Sensing (CHRS), The Henry Samueli School of Engineering, Department of Civil and Environmental Engineering, University of California, Irvine, CA 92697, USA
- ^b Water Engineering Department, Shiraz University, Shiraz 71964-84334, Iran
- c Department of Meteorology, Faculty of Marine Science and Technology, Tehran North Branch, Islamic Azad University, Tehran 1651153311, Iran
- ^d Department of Earth System Science, University of California Irvine, 3200 Croul Hall, Irvine, CA 92697-2175, USA

ARTICLE INFO

This manuscript was handled by Emmanouil Anagnostou, Editor-in-Chief, with the assistance of Pierre-Emmanuel Kirstetter, Associate Editor

Keywords: Remote sensing Heavy precipitation CONNECT algorithm PERSIANN-CCS MERRA-2

ABSTRACT

In recent years, the number of floods following unprecedented rainfall events have increased in Iran during early spring (March 21st to April 20th, referred to in Iran as the month of "Farvadin"). While numerous studies have addressed changes in climate extremes and precipitation trends at different temporal scales from daily to annual across the country, analyses of short-duration and heavy precipitation, especially during recent years, are rarely considered. Furthermore, most studies investigate the variations in extremes and total precipitation using a limited number of synoptic weather stations across Iran. This study assesses the variations in heavy precipitation (precipitation with intensities greater than or equal to 3 mm/3 h) at 0.04° spatial and 3-hourly temporal resolution during the month of Farvardin. In addition, the effect of atmospheric river conditions over Iran and their possible link to intensifying heavy precipitation is explored. For this purpose, the CONNected-objECT (CON-NECT) algorithm is applied on a precipitation dataset, Precipitation Estimation from Remotely Sensed Information Using Artificial Neural Networks-Cloud Classification System (PERSIANN-CCS), and an Integrated Water Vapor Transport (IVT) dataset from the NASA Modern-Era Retrospective Analysis for Research and Applications Version-2 (MERRA-2). The results suggest that the increase in the number of floods in recent years is related to the increase in the intensity and volume of heavy precipitation events, although the frequency and duration of heavy precipitation events have not changed significantly. Furthermore, the results show that atmospheric river conditions over the country are present during the same window as each year's most extreme events. It is found that 8 out of 13 of the largest ARs over Iran come from moisture plumes with pathways over the African and Red Sea.

1. Introduction

Over the 2018–2020 period, Iran experienced several unprecedented precipitation events that caused devastating floods across the country during the first month of spring (referred to as the month of "Farvardin", spanning from March 21st to April 20th). During Farvardin 2019, Iran was hit by three major waves of extreme precipitation events, which led to flooding in 26 of Iran's 31 provinces. According to the International

Disaster database (www.emdat.be), these widespread major floods caused \$3.5 billion (2019 USD) in economic damages and more than 78 fatalities (Aminyavari et al., 2019; Asanjan et al., 2019). Inundations and landslides also damaged 8,700 miles (one-third) of Iran's roads and completely destroyed more than 700 bridges (Bozorgmehr, 2019). Heavy rainfall during Farvardin 2020 caused damage to large areas in 18 provinces of the country. More than 11 people lost their lives and the total economic damages were in excess of \$2.2 billion (United Nations

E-mail address: mojtabas@uci.edu (M. Sadeghi).

^{*} Corresponding author.

Office for the Coordination of Humanitarian Affairs, https://www.unocha.org/).

Due to these recent catastrophic flooding events, there is a need to better understand the variability in precipitation intensity, frequency, and mechanisms of precipitation in early spring over Iran. There are several studies that have investigated the spatial and temporal variations of precipitation over Iran at different temporal scales using a synoptic gauge dataset with different data record lengths (Boroujerdy, 2008; Feizi et al., 2014; Javari, 2016; Kousari et al., 2011; Najafi and Moazami, 2016; Raziei et al., 2014; Shirvani, 2017; Some'e et al., 2012; Tabari et al., 2011; Zarenistanak et al., 2014). For example, Modarres et al. (2007) studied the precipitation variability over Iran by analyzing annual precipitation data collected from 20 gauge stations for the period from 1955 to 2000. Of those 20 stations, 18 showed no statistically significant trends in precipitation. Tabari et al. (2011) conducted a study to investigate the variations in annual and seasonal precipitation using 61 synoptic stations for the period from 1966 to 2005. Their results indicated that the amount of annual precipitation decreased significantly over time at about 60% of the stations. Similarly, they showed that trends for the spring and winter precipitation were mostly negative during the study period. Soltani et al. (2012) applied the Mann-Kendall test to the annual and monthly rainfall time series of 33 synoptic stages for the period from 1951 to 2005. By analyzing the annual precipitation, they concluded that there was no significant climate change overall in Iran, specifically in March rainfall, while significant negative trends were noticed at 29 stations in April. More recently, an investigation by Zarei and Masoudi (2019) of precipitation variations based on 40 stations during the time period from 1967 to 2014 revealed that about 30% of the stations showed significant decreases in annual precipitation.

Although the spatiotemporal variability of precipitation over Iran is investigated by these studies, there are still some notable gaps: First, these studies analyze a limited number of synoptic weather stations, making it difficult to understand precipitation variation at high spatial resolution over the whole country. Furthermore, urbanization over recent decades may have affected the station data trends. Second, the synoptic gauge precipitation network provides precipitation observations at a daily time scale. This temporal resolution limits the focus of the studies to the total amount of precipitation at daily to annual scales. Therefore, the variations in heavy precipitation at sub-daily scales (e.g. hourly, 3-hourly) were not explored. Third, the temporal extent of these studies spans to the year 2013, meaning the unprecedented rainfall events during Farvardin over the 2018–2020 period have not been examined.

The inadequate and sparse networks of rain gauge stations across Iran increase the uncertainties in previous study findings. Additionally, the daily temporal resolution of rain gauge networks undermines their applicability to capture the variations in short-duration heavy precipitation events (Maggioni et al., 2016; Mosaffa et al., 2020a, 2020b, 2020c; Yang et al., 2005). Satellite-based precipitation estimates are a promising alternative to ground-based rain measurements, offering global precipitation estimates with high spatial and temporal resolution, especially over sparsely gauged regions (Sadeghi et al., 2020, 2021).

Precipitation Estimation from Remotely Sensed Information Using Artificial Neural Networks-Cloud Classification System (PERSIANN-CCS), which provides near-real time precipitation estimates at 0.04° spatial resolution an0d hourly temporal resolution, is an attractive candidate for short-duration extreme precipitation analysis (Hong et al., 2004). Many studies have evaluated the estimation performance of PERSIANN-CCS at global to local scales (Beck et al., 2019; Bitew and Gebremichael, 2010; Conti et al., 2014; Hirpa et al., 2010; Hong et al., 2007; Hsu et al., 1997; Katiraie-Boroujerdy et al., 2020; Romilly and Gebremichael, 2011; Asanjan, et al., 2019; Salmani-Dehaghi and Samani, 2019). Over Iran, Mosaffa et al. (2020a), Mosaffa et al. (2020b) and Mosaffa et al. (2020c) evaluated the near-real time precipitation estimation products, including PERSIANN-CCS and Tropical Rainfall Measuring Mission real-time (TRMM 3B42-RT), comparing these

products against 28 rain gauge observations for the period from 2003 to 2014. Their results showed that PERSIANN-CCS performed better in terms of both rainfall detection and estimation compared to TRMM 3B42-RT. Katiraie-Boroujerdy et al. (2020) evaluated PERSIANN-CCS against 1,130 rain gauge stations over Iran for the period from December 2008 to November 2018 and showed that PERSIANN-CCS estimates are consistent with gauge observations. In this study, we leverage the high-spatiotemporal resolution PERSIANN-CCS dataset to investigate the variation of short-term heavy precipitation in the month of Farvardin over the last two decades (2003–2020). This study highlights the application of near-global PERSIANN-CCS estimates for exploring precipitation variation over countries where the number of rain gauges is limited, like Iran.

Iranian agriculture is highly dependent on precipitation in spring, especially that in the month of Farvardin, the first spring month in the Iranian calendar. According to PERSIANN-CCS measurements, approximately a quarter of the annual precipitation in Iran occurs during Farvardin. The consequences of climate change on the intensification of the hydrologic cycle, including floods and droughts, caused many heavy precipitation events in recent years. For example, according to Iranian agriculture ministry's crisis management department, flooding in multiple Iran provinces during Farvardin 2019 caused nearly \$3 billion to the agriculture sector (https://www.tehrantimes.com/news/434705/). Among those provinces, early spring floods caused financial damages amounting to approximately \$714 million to 200,000 ha of Khuzestan farming lands alone.

In this study, we use PERSIANN-CCS estimates to address the gaps in the previous studies for investigating heavy precipitation events during the month of Farvardin over Iran. First, the high spatial resolution of the PERSIANN-CCS estimates enables us to investigate the variations in precipitation at 0.04° spatial resolution. Second, the hourly temporal resolution of the PERSIANN-CCS estimates provides us the opportunity to explore the variations in short-duration extreme precipitation. For this purpose, this study utilizes the CONNected objECT (CONNECT) algorithm run on the PERSIANN-CCS estimates, which is an objectoriented tracking algorithm, to investigate the spatiotemporal variations in short-term heavy precipitation during the month of Farvardin over Iran using the PERSIANN-CCS dataset as input. In this study, we consider 3 mm/3 h as the threshold precipitation rate to determine heavy precipitation. This study highlights the application of the CON-NECT algorithm along with PERSIANN-CCS dataset for analyzing natural hazards associated with AR events, such as floods over different regions of the globe.

To further explore the spatiotemporal variations of heavy precipitation events during Farvardin, we examine the presence of atmospheric rivers (ARs) over the country and during periods of extreme precipitation. The spatial distribution of precipitation over Iran is mostly affected by the interaction of large-scale atmospheric circulation types and the Zagros and Alborz Ranges. Some particular meteorological conditions, such as the position of mid-tropospheric ridges, troughs, and the jet stream, along with ARs that bring moisture from faraway water bodies, are pushed upward by orography and produce precipitation over Iran in early spring (Alijani, 2002; Azizi et al., 2013; Vaghefi et al., 2019). The effective synoptic conditions for spring precipitation in Iran are mainly driven by the interconnection and positioning of the Mediterranean low pressures, the Siberian high pressure, the Red sea, and the Arabian low-tropospheric anticyclones (Alijani and Harman, 1985; Darand and Daneshvar, 2014; Nazaripour and Daneshvar, 2014).

Thus far, there has been minimal insight into how ARs contribute to heavy precipitation that occurs during the early spring across the country. Recently, Dezfuli (2019) investigated the mechanisms of ARs over the Middle East by examining the unprecedented precipitation event that occurred during March 24–25, 2019. Their results indicated that the strong, nearly 9000-km-long AR Dena that was propagated from the Atlantic Ocean and was fed by additional moisture from surrounding bodies of water along its pathway was responsible for this

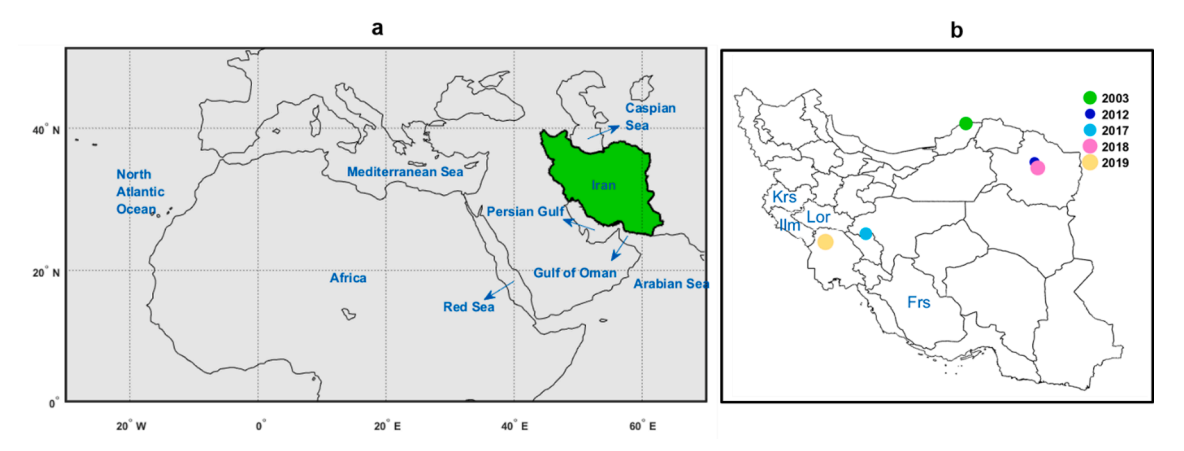


Fig. 1. a) The study area (green) and surrounding regions b) Selected provinces including Ilam (Ilm), Fars (Frs), Kermanshah (Krs), and Lorestan (Lor) and location of the five heaviest events in Farvardin in terms of volume (2003, 2012, 2017, 2018, and 2019) that are discussed in Figs. 7 and 8. (For interpretation of the references to colour in this figure legend, the reader is referred to the web version of this article.)

unprecedented precipitation. In this study we leverage the CONNECT algorithm to further examine the presence and therefore implied influence of ARs during the most extreme precipitation events that have occurred during the month of Farvardin during the last two decades.

The detailed goals of this study are:

- 1- Investigate the temporal variations in heavy precipitation events that occurred in the month of Farvardin from 2003 to 2020 using PERSIANN-CCS estimates.
- 2- Explore AR conditions over Iran, especially during heavy precipitation events that occurred during the last two decades.
- 3- Explore the applications of the CONNECT with PERSIANN-CCS for tracking short-term precipitation events.
- 4- Investigate the performance of PERSIANN-CCS for the precipitation events behind Iran's major floods in 2019.

The rest of this paper is organized as follows. In the next section, we describe the datasets (precipitation and Integrated Water Vapor Transport, hereafter "IVT") which are used in this study. In Section 3, we briefly describe the CONNECT algorithm and the methodology used to analyze the variations in heavy precipitation during Farvardin. Results are presented in Section 4. We summarize the major findings of this study and conclude this paper in Section 5.

2. Study area & data

2.1. Study area

Iran is in a semi-arid and arid subtropical region of southwest Asia at longitude 25–40°N and latitude 44–65°E. The country is bounded by the Caspian Sea on the north and the Persian Gulf and Gulf of Oman in the south (Fig. 1). The study area covers the extent of Iran's borders, measuring at about 1.6 million km². Iran is characterized by complex topography: most of the central and southeastern parts of Iran are covered by barren/arid areas (Dashte-e Kavir and Dashte-e Lut) and western and northern regions are covered by Zagros and Alborz main mountain ranges. Iran is the scene of various meteorological and climatological mechanisms (mostly induced by the subtropical highpressure regimes) resulting in uneven spatial and temporal distribution of precipitation across the country. The southern part of Iran is affected by the anticyclonic circulation over the Arabian Sea (Raziei et al., 2012), the El Niño-Southern Oscillation (ENSO) (Nazemosadat and Ghasemi, 2004; Saghafian et al., 2017), and the Monsoon phenomenon (Yadav, 2016; Zarrin et al., 2010) while mountainous regions in western Iran block moisture-loaded ARs from the tropical Atlantic Ocean and Europe driven by the Black Sea and Mediterranean cyclones

(Azizi et al., 2013; Vaghefi et al., 2019)

In our study, to identify the spatial and temporal variations of heavy precipitation events during the month of Farvardin and examine the effect of ARs on these variations, we consider a large spatial domain from 10° W to 70° E and from 0° to 50° N, including some parts of North Atlantic Ocean, Europe, Middle East, and North Africa (Fig. 1).

2.2. Data sets

• PERSIANN-CCS

PERSIANN-CCS is a satellite-based operational product that consists of hourly rainfall estimates at $0.04^{\circ} \times 0.04^{\circ}$ (approximately 4 km) spatial resolution (Hong et al., 2004). It uses infrared (IR) imagery from geostationary satellites and extracts the cloud features such as temperature, geometry, and texture to estimate rainfall using a data-driven model. PERSIANN-CCS is a useful tool for monitoring and analyzing heavy precipitation events in near-real-time at a quasi-global scale (60°N to 60°S). This dataset is available as an operational climate data record via the CHRS Data Portal (http://chrsdata.eng.uci.edu/, Nguyen et al., 2019).

• PERSIANN-CDR

PERSIANN-Climate Data Record (CDR), like PERSIANN-CCS, is a rainfall product that is a quasi-global and satellite-based. PERSIANN-CDR differs from PERSIANN-CCS by its intention: while PERSIANN-CCS is primarily for real-time measurements, PERSIANN-CDR's long duration (1983-present) makes it most useful for climate-scale studies (Ashouri et al., 2015; Sadeghi, 2018; Sadeghi et al., 2019a, 2019b). As accuracy is a primary motivation for the development of PERSIANN-CDR data, daily passive microwave data and monthly GPCP v2.3 rain gauge values are used for bias correction. PERSIANN-CDR's focus on accuracy means it's not available at scales as fine as PERSIANN-CCS—PERSIANN-CDR's spatiotemporal resolution is limited to daily and $0.25^{\circ} \times 0.25^{\circ}$ pixels. In this study, PERSIANN-CDR is used to investigate the climatology of AR-associated rainfall during Farvardin. Like PERSIANN-CCS, PERSIANN-CDR is available from the CHRS Data Portal (see above.)

• Integrated Water Vapor Transport from MERRA-2

Integrated water Vapor Transport (IVT) is the amount of atmospheric moisture integrated across all levels of the atmosphere, calculated from the following formula:

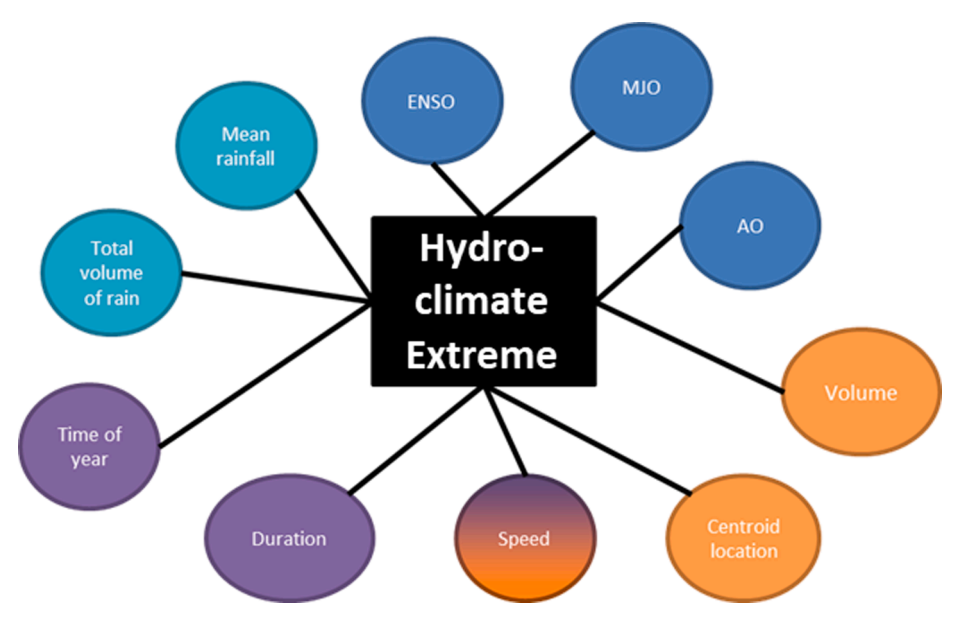


Fig. 2. An object ("hydroclimate extreme") described by its characteristics ("total volume of rainfall", "duration", etc.)

$$IVT = \frac{1}{g} \int_{P_{\text{mod}}}^{P_{200}} qV dp$$

where p is pressure (hPa), p_200 is pressure at 200 hPa, assumed to be the top of the atmosphere, p_surf is the geopotential height at the Earth's surface (1000 hPa), q is specific humidity at pressure height p, Vis the wind velocity (m/s) at p, and g is gravitational acceleration. IVT was calculated from the wind and pressure values retrieved from the National Aeronautical and Space Agency's (NASA) Modern-Era Retrospective Analysis for Research and Applications-version 2 (MERRA-2) data (Gelaro et al., 2017).

· Gauge dataset

To evaluate PERSIANN-CCS's accuracy during Farvardin 2019, the PERSIANN-CCS estimates are compared with ground-based gauge observations from 70 synoptic meteorological stations from the Iran Meteorological Organization at the daily scale. These evaluations are performed over 4 provinces (Fars, Lorestan, Kermanshah, and Ilam) which were affected the most by the heavy precipitation events during Farvardin 2019. The comparison is conducted against PERSIANN-CCS pixels that contained at least one meteorological ground-based observation.

3. Methodology

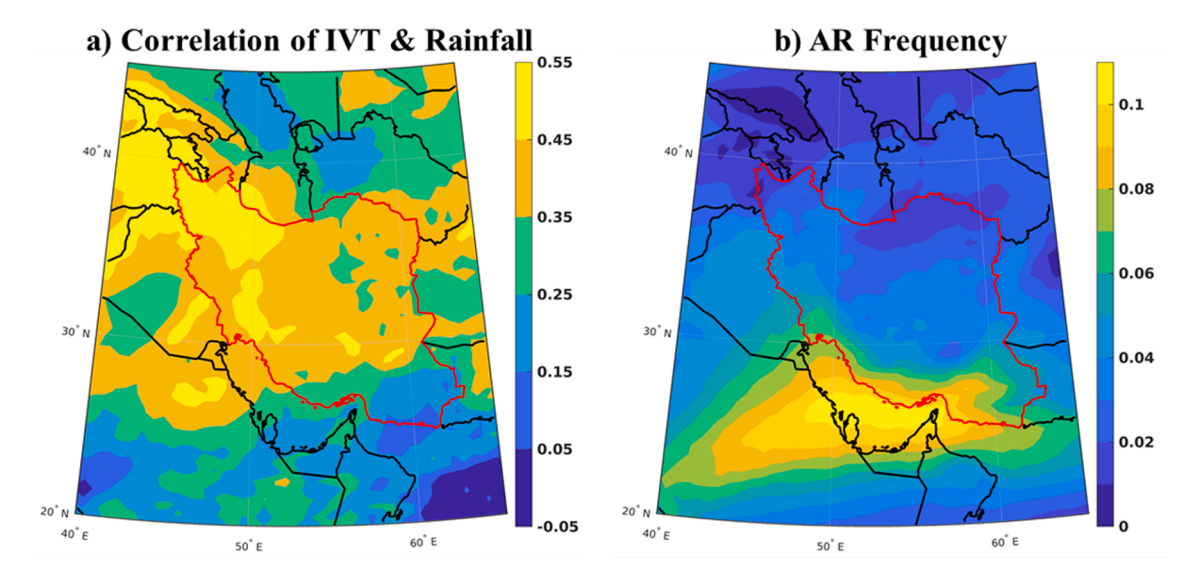
3.1. CONNECT

The CONNected-objECT (CONNECT) algorithm is a big data algorithm that uses connectivity (overlap) to segment, group, and track elevated or anomalous data signatures in large volumes of data. It was developed to study hydroclimate extremes, including, but not limited to, ARs (Shearer et al., 2020), tropical and extratropical cyclones (Shearer et al., 2021), droughts, and more. The algorithm's architecture is designed with object-oriented analysis in mind, where "objects" are identified items, events, etc. that can be represented by attributes and statistics and object-oriented analysis is the study of populations of "objects" from their attributes and statistics (Fig. 2). Object-oriented analysis has noteworthy benefits for hydroclimate studies: events are discretely counted and recorded, meaning they can be examined individually, or their population considered statistically, from techniques as simple as calculating averages and percentiles to distribution building

and cluster analysis.

CONNECT uses three-dimensional (x,y-spatial and temporal) voxels of a target variable (e.g. rainfall) to construct objects where voxels with intensities above a user-defined threshold are contiguous over space and time, performed using a flood filling algorithm. As grouping voxels across the time axis captures the evolution of an object from genesis to terminus, CONNECT performs well as a tracking algorithm, meaning objects segmented by CONNECT are the lifecycles of weather phenomena. CONNECT auto-calculates object characteristics, such as spatiotemporal properties like volume, speed, duration, etc. and outputs it into a table for statistical/object-oriented analysis.

For this study, 3-hourly precipitation data from PERSIANN-CCS during the month of Farvardin every year from 2003 to 2020 was used as input to CONNECT. As our interest for this study lies entirely within the boundaries of Iran, precipitation fields are clipped to the country's borders. To capture longer-duration heavy events over the region, CONNECT was set up to only consider rainfall totals equal to or greater than 3 mm/3 h and to filter objects with durations shorter than twelve hours. Selecting the threshold parameter for CONNECT is largely based on balancing between over-segmenting and under-segmenting. Over-segmented rainfall disrupts the tracking functionality of CON-NECT: smaller objects moving at faster speeds will not overlap during subsequent timesteps and will not be considered as the same object. At the same time, under-segmented rainfall will track multiple events as a singular "conglomerate" event. As an example, consider rainfall systems in the intertropical convergence zone. At very low thresholds, CONNECT will not differentiate between the light rainfall that constantly occurs in the region and the periodic heavy rainfall from transient mesoscale convective systems that also frequently form and dissipate over the course of a day. If a researcher's goal is to study the lifecycles of the latter phenomena, a higher rainfall threshold rate is required for suitable results. We note similarities between the geography of Iran and California (further explained in the subsequent section) and therefore elect to use the 1 mm/hour (here, 3 mm/3-hour) threshold used in Sellars et al. (2015). At this value, rainfall is a less than half of the Glossary of Meteorology's definition of moderate rainfall (2.5 mm/hour), but well above the rainfall rates of a drizzle (0.3 mm/hour), meaning rainfall rates captured are impactful but not necessarily extreme. A higher threshold is undesirable as it omits important data and serves to underestimate storm total volume calculations.



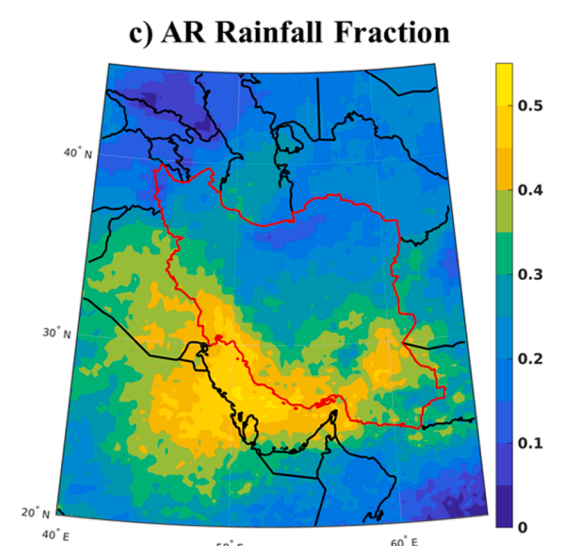


Fig. 3. Climatology of ARs over Iran during Farvardin, using 1990–2019 baseline period. a) The correlation of 24-hr (00z-00z) IVT averages to 24-hr precipitation accumulations from PERSIANN-CDR. b) Frequency of AR conditions. c) Fraction of precipitation.

3.2. Defining the thresholds for detecting AR over Iran.

An AR is a narrow, transient atmospheric pathway that transports a large amount of water vapor from distant water bodies. In dry countries like Iran, which is located in subtropical latitudes, ARs originating from water bodies located west of the country can be a significant source of precipitation. Furthermore, Guan and Waliser (2015) showed that ARs are contribute to orographic rainfall occurrences and can cause extreme precipitation events and flooding in Iran. Therefore, for hydrological purposes it would be useful to study extreme precipitation events

and ARs particularly in mountainous region of Iran (e.g, Zagros Range). To investigate whether the most extreme CCS-CONNECT objects over Iran were related to AR activity, we utilized the methodology from Rutz et al. (2014, hereby referred to as "Rutz"). Rutz defines an AR as a region of IVT greater than 250 $kgm^{-1}\ s^{-1}$ that extends to a length greater than or equal to 2,000 km. The Rutz methodology is referred to as a "permissive" methodology (as opposed to a "restrictive" method), which means its requirements are laxer and generally tend to classify anomalous IVT regions as ARs more often than other methodologies. This methodology was selected because Iran has notable analogs to California, where the methodology was developed, including its northwest-southeast trending Zagros Mountain range with peaks up to 4,400 m,

which has the same orientation and prominence as the Sierra Nevada Range, along with its location in the lower mid-latitudes. However, we acknowledge that Iran's position east of the dry Saharan Desert is in stark contrast to California's proximity west of the Pacific Ocean, a water body source which feeds Pacific ARs with their moisture, though a notable analog exists in the Red and Mediterranean Seas, along with the Persian Gulf (Dezfuli, 2019). Furthermore, ARs over Iran have yet to be analyzed using an precipitation-linked IVT threshold which can be utilized in global studies, like that used in Rutz et al., (2014); the 85th percentile of IVT over Iran and the surrounding region was used as a threshold in Dezfuli (2019) and Esfandiari and Lashkari (2020), the values of which would be far too low of a threshold to be useful over North America, Europe, etc. It is important to note that we do not argue that using a regionally derived IVT threshold makes the ARs in these studies less deserving of the AR label. However, by proving that ARs exist at IVT levels that can be utilized globally and is tied to precipitation, we prove that Iran is a region where ARs of noteworthy strength frequently occur, at least in the month of Farvardin, making it comparable to the North American west coast, Europe, Chile, and other regions

To robustly investigate the influence ARs have in the region during Farvardin, the climatology of ARs and AR precipitation over Iran during

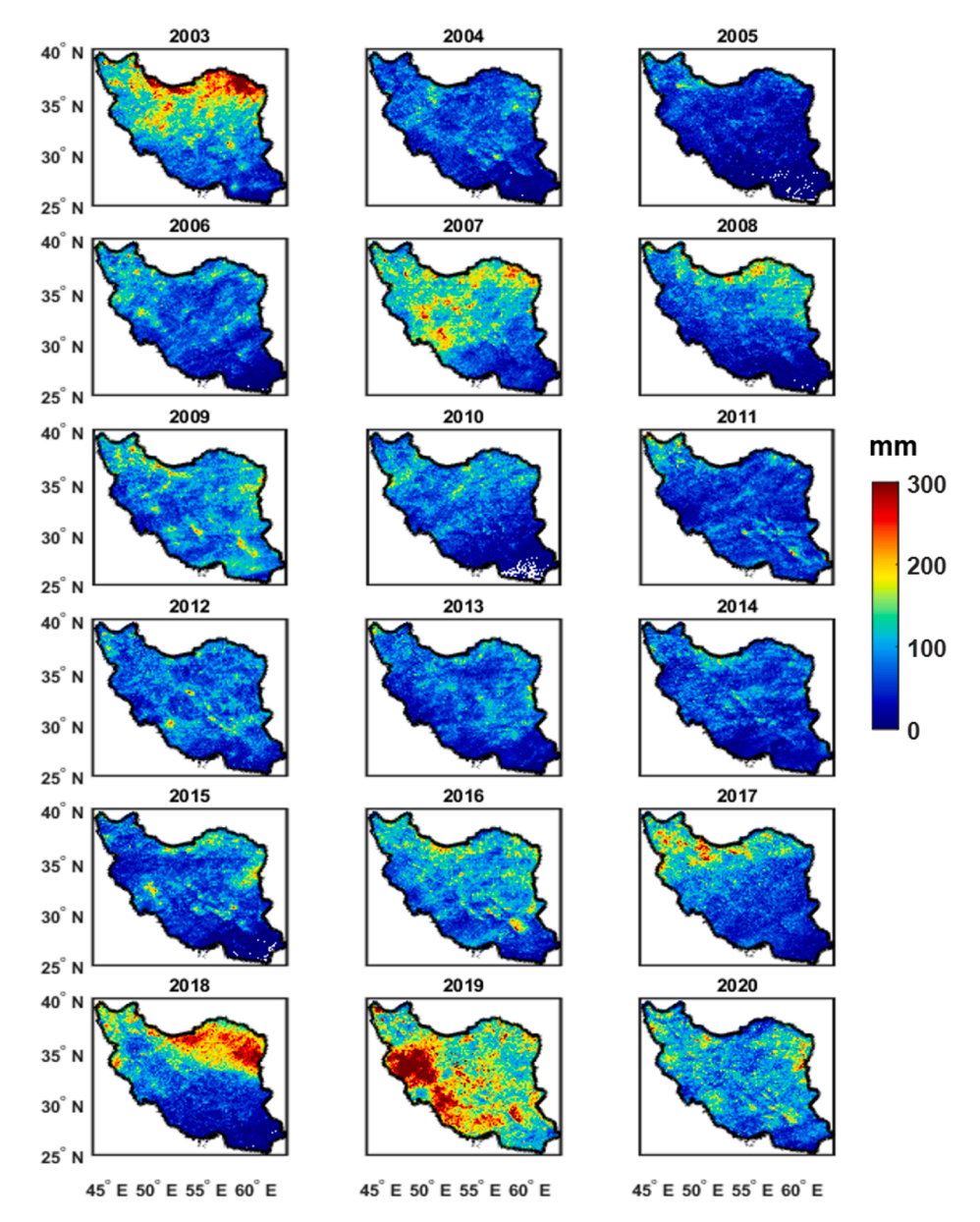


Fig. 4. Accumulated precipitation estimates for the month of Farvardin over Iran from 2003 to 2020 using PERSIANN-CCS estimates.

the month of Farvardin is investigated using the Rutz methodology and the multi-decade PERSIANN-CDR precipitation dataset over 1990-2019. The 30-year duration was chosen in compliance with the standards of the World Meteorological Organization (WMO). Fig. 3 explores three metrics that seek to investigate how ARs impact Iran during Farvardin, specifically regarding frequency and its link to precipitation. In the Zagros mountains, precipitation and IVT are correlated to values as high as 55%, including the greater Tehran metropolis. Moreover, moderate correlations of 35%-45% exist across the entirely of north and central Iran. AR frequencies are greatest along the coast of the Persian Gulf and the Gulf of Oman up to the foot of the Zagros Mountains, where they occur on average 7-10% of the month, or up to 3 days a month. Thus, two similarities between the climatology of Iran and California are observed: the high correlation between IVT and rainfall, especially in topographically complex regions (Rutz et al., 2014) and the high frequency of elevated IVT fluxes that perpendicularly strike a prominent mountain range. In addition, the fraction of AR rainfall is over 50% in the southern part of the country. Owing to these similarities, it can established that 1) atmospheric rivers at IVT fluxes required by the Rutz methodology (impact-linked) are non-insignificant players in Iran's Farvardin hydroclimate, meaning 2) The Rutz methodology and others that aren't linked to climatological averages, like what is done in Defuzli (2019), are appropriate to use in the region for AR-related studies. In this study, we investigate the contribution of ARs on heavy precipitation using IVT and gauge information.

Despite the breadth of analysis done in this study regarding ARs over Iran and their perceived link to heavy precipitation events, it is vital to note that establishing a concrete link between ARs and heavy precipitation requires numerical modeling simulation as described by Davolio et al. (2020) and such research should be conducted before solid conclusions can be made. Such numerical simulations are outside the scope of this study.

3.3. Performance measurements

Categorical evaluation statistics including Probability of Detection (POD), False Alarm Ratio (FAR), Critical Success Index (CSI) are utilized to evaluate the performance of the PERSIANN-CCS dataset for detecting rain/no rain pixels. Continuous indices including Pearson's correlation coefficient (CC), Root Mean Square Error (RMSE) and Bias (BIAS; BIAS

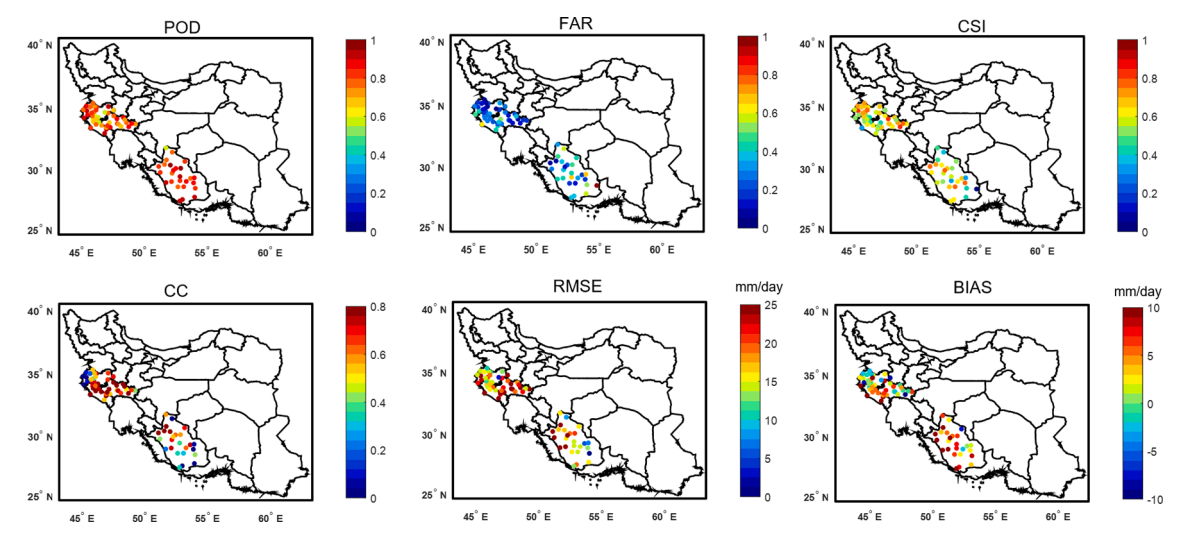


Fig. 5. Spatial distribution of different statistical evaluation metric over the four selected provinces.

= estimation-observation) are used to assess the accuracy performance of PERSIANN-CCS in estimating the rainfall intensity. A value of 1 mm/day is utilized as a rain/no rain threshold in both PERSIANN-CCS estimates and ground-based gauge observations.

4. Results and discussion

Fig. 4 displays the spatial map of the accumulated precipitation for the month of Farvardin during the period from 2003 to 2020 using PERSIANN-CCS data. The mean monthly precipitation during Farvardin for this period was 86 mm. For the most recent years, the average precipitation was 107 mm (in 2018), 178 mm (in 2019), and 100 mm (in 2020), all of which were higher than the baseline mean precipitation from 2003 to 2020. Furthermore, the year 2019, when Iran experienced

many floods, was the wettest year in the last two decades. In addition, Fig. 4 reveals that the spatial pattern of accumulated precipitation varies among different years. The greatest concentration of rainfall occurred over northeastern Iran in 2003 while southwestern Iran experienced the bulk of precipitation in 2019.

4.1. Evaluation of PERSIANN-CCS for 2019

As discussed in the introduction, Katiraie-Boroujerdy et al. (2020), Mosaffa et al. (2020a), Mosaffa et al. (2020b) and Mosaffa et al. (2020c) evaluated the performance of the daily PERSIANN-CCS estimates over Iran for the period prior to 2018. The intention of this study is not to evaluate the capability of PERSIANN-CCS for precipitation estimation, but rather evaluate rainfall totals during Farvardin 2019 against ground-

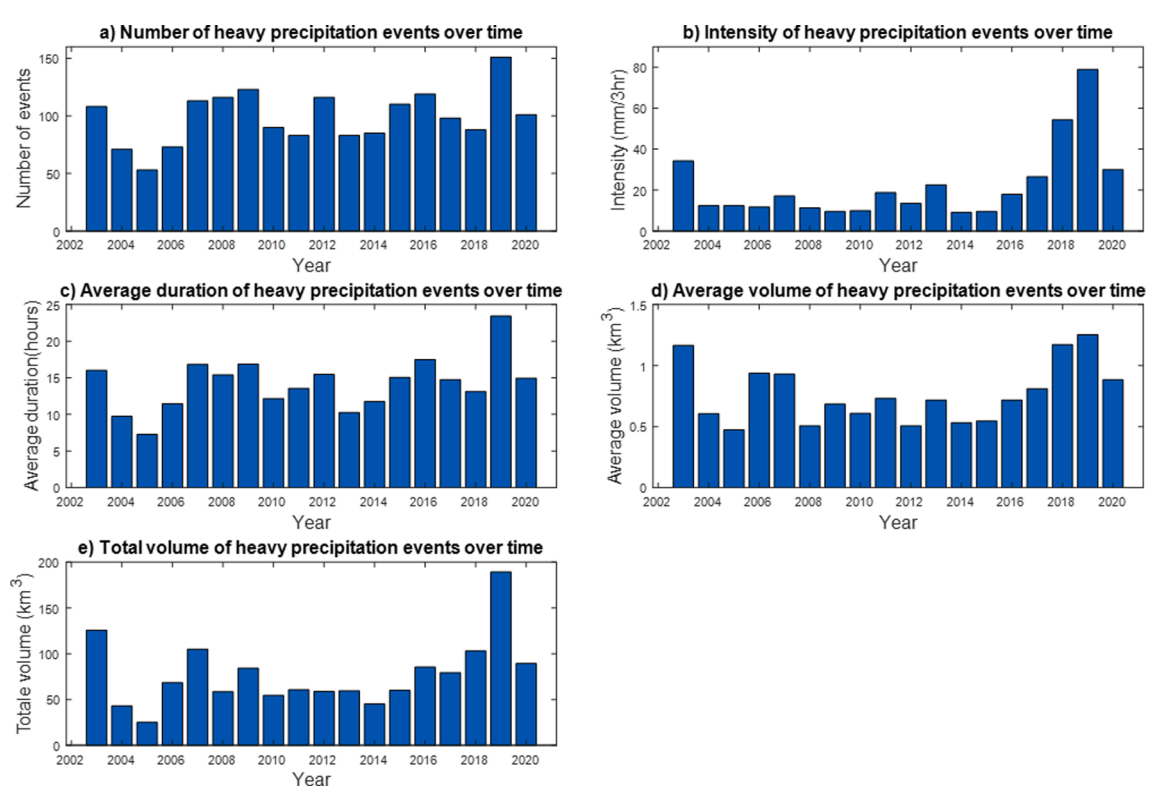


Fig. 6. Temporal variations of heavy precipitation events during the period 2003-2020 using PERSIANN-CCS estimates.

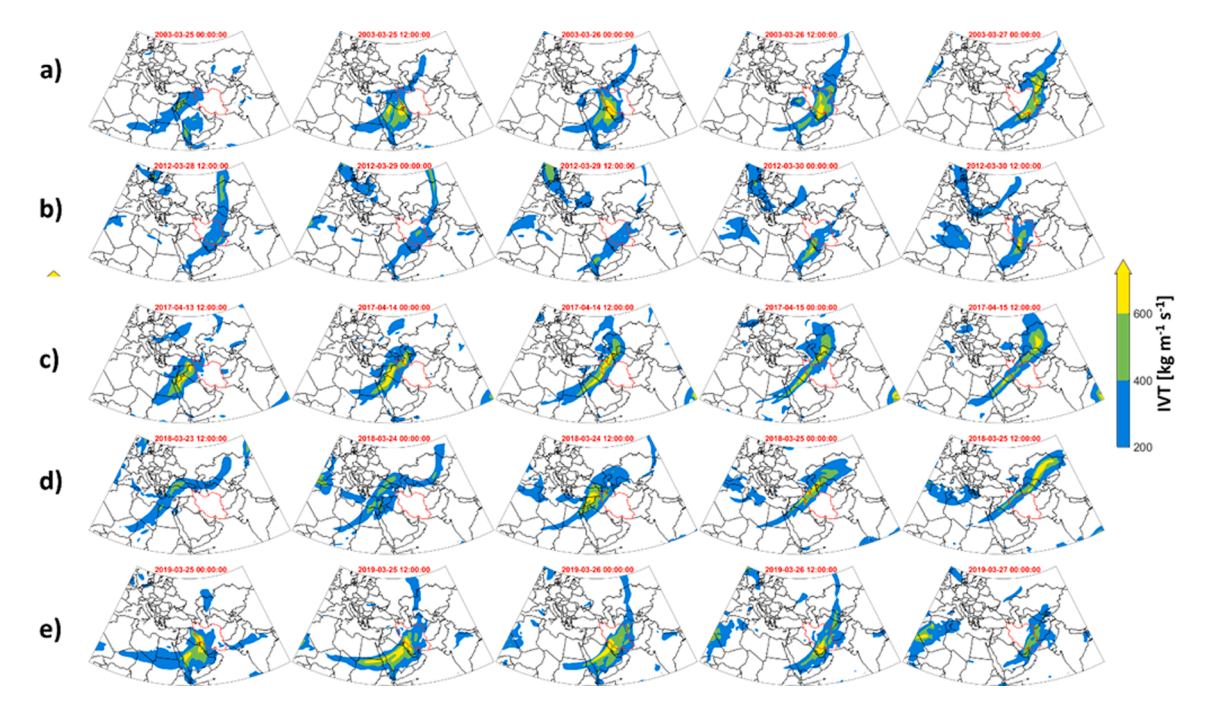


Fig. 7. AR presence during the most severe heavy precipitation events during 2003–2020: a) 2003 b) 2012 c) 2017 d) 2018 e) 2019.

based observations for the provinces that experienced floods. Table 2 presents spatial averages of categorical and continuous evaluation metrics over four selected provinces: Fars, Ilam, Kermanshah, and Lorestan. These are among the provinces that reported the greatest flooding damages during the Farvardin 2019 floods. In terms of categorical statistics, POD and FAR values are 0.78 and 0.28 over these provinces, respectively. PERSIANN-CCS with 0.65 (0.53) has the best (worst) performance in terms of CSI over Kermanshah (Ilam) province. According to continuous statistical metrics, the correction coefficient (CC) is approximately 0.55 in the selected provinces and the highest CC values appear over the Ilam province with the value of 0.75. Also, RMSE ranges from 16.55 to 23.14 mm/day. In terms of bias, PERSIANN-CCS mainly overestimates (BIAS > 0) precipitation intensity. When comparing our results to those of previous studies which evaluated different satellite precipitation products over Iran (Alijanian et al., 2017; Mahbod et al., 2019; Moazami et al., 2013; Mosaffa et al., 2020b, 2020c), it must be pointed out that PERSIANN-CCS performs better than other near-real time products during Farvardin 2019.

Fig. 5 presents the spatial distribution of POD, FAR, CSI, CC, RMSE, and BIAS over the four selected provinces. This figure shows that POD values in all stations is above 0.75 except a station in the north of Fars province and a couple of stations in the middle of western provinces which have POD about 0.6. Western provinces including Kermanshah, Ilam, and Lorestan have lower FAR than the Fars province in the south of Iran. Except for a few stations with CSI below 0.5, mostly found in the Fars province, other stations have CSI greater than 0.5. The spatial distribution of CC indicates that the PERSIANN-CCS algorithm has better performance over the western provinces than over Fars. According to Fig. 5, CC in regions that experienced heavier precipitation is higher than in the other regions. Stations in the Lorestan province have the highest RMSE compared with other stations. On the contrary, stations in the south of Fars and Kermanshah provinces have the lowest RMSE. Although precipitation is overestimated (BIAS > 0) in most of the stations, results of BIAS in the north of the Kermanshah province and a couple of stations in the east of the Lorestan province shows an underestimation of precipitation. Comparing with the conducted evaluation studies for near-real time precipitation over Iran, PERSIANN-CCS has the potential to be used as a candidate for short-term duration precipitation studies.

4.2. Temporal variations of heavy precipitation events during the period 2003–2020 using PERSIANN-CCS estimates

To quantify how the number of floods has been increasing during the last three years, we plot the frequency, intensity, duration, and volume of precipitation for the period 2003-2020 over the study area (Fig. 6). For this purpose, we apply the CONNECT algorithm with a 3 mm/3-hour threshold on the PERSIANN-CCS estimates for the period 2003–2020 for the month of Farvardin across Iran. The frequency (Fig. 6a) of heavy precipitation events—events with more than 3 mm/3-hour rainfall—does not show a significant change across the country during the month of Farvardin. The average number of intense events is 97; however, the highest number is 151 events occurring in 2019. The variations in intensity of heavy precipitation events (Fig. 6b) demonstrate that the average magnitude of heavy rainfall has increased during the last three years. The average intensity of heavy precipitation events is 15.7 mm/3hour for the whole period compared with 55.3 mm/3-hour in 2018, 79.0 mm/3-hour in 2019, and 30.1 mm/3-hour in 2020. These results are consistent with the increase in the number of floods reported across Iran during the last three years. The average duration of heavy precipitation (Fig. 6c) was 14.2 h during the last two decades, while peaking to 23.8 h in 2019. The average volume of heavy precipitation (Fig. 6d) during the month of Farvardin for the whole study period is 0.7 km³/ event, while an average of 0.97 km³/event was recorded over the last three years of the study. The total volume of heavy precipitation per year (Fig. 6e) was 77 km³ on average, compared with an average of 132 km³ of precipitation occurring during the last three years. Most notably, the total precipitation volume was 191 km3 in 2019. Overall, we can conclude that the increase in intensity, average volume per event, and total volume of heavy precipitation are the main reasons for the increases in the number of floods during the last three years over Iran.

4.3. Investigating atmospheric river presence during heavy precipitation events from 2003 to 2020

The Rutz et al. (2014) methodology was used to determine whether there was AR activity during the most extreme Farvardin rainfall events every year during 2003–2020, including extra significant events in 2019 and 2020. As Rutz is considered a permissive methodology, which

Table 1 Statistical evaluation of daily PERSIANN-CCS over selected provinces.

	Average on selected Province	Fars Province	Ilam Province	Kermanshah Province	Lorestan Province
POD	0.78	0.83	0.71	0.76	0.79
FAR	0.28	0.37	0.32	0.18	0.21
CSI	0.60	0.55	0.53	0.65	0.64
CC	0.62	0.48	0.75	0.47	0.69
RMSE (mm/ day)	19.97	20.10	21.95	16.55	23.14
BIAS (mm/ day)	3.44	6.38	6.31	0.96	1.37

Table 2The heaviest precipitation events during 2003–2020 and the presence of ARs bringing moisture over north Africa ("Af") or the Red Sea ("RS") during the event period.

Date	AR?	>24 Hours	Pathway	Rainfall Volume (km³)	Rank
22 March–26 March 2003	Yes	Yes	Af & RS	34.22	4
April 1–April 6, 2004	Yes	Yes	Af & RS	12.49	13
April 13–April 19, 2005	Yes	Yes	RS	12.33	14
27 March-31 March 2006	Yes	Yes	RS	11.71	15
24 March–27 March 2007	Yes	Yes	Af & RS	17.09	10
April 6–April 10, 2008	Yes	Yes	Af & RS	11.25	16
29 March–2 April 2009	Yes	Yes	Gulf of Aden	9.48	20
26 March–29 March 2010	Yes	No	RS	9.87	17
3 April–8 April 2011	Yes	No	Af & RS	18.71	8
26 March–31 March 2012	Yes	Yes	RS	13.48	11
4 April–8 April 2013	Yes	No	Arabian Sea	22.53	7
1 April–4 April 2014	Yes	Yes	Af & RS	9.07	21
28 March-1 April 2015	Yes	Yes	Af & RS	9.51	19
11 April–15 April 2016	Yes	Yes	Af & RS	12.91	12
23 March–28 March 2016	Yes	Yes	Af & RS	17.94	9
12 April–16 April 2017	Yes	Yes	Af	26.57	6
21 March–26 March 2018	Yes	Yes	Af	54.29	2
22 March–27 March 2019	Yes	Yes	Af & RS	78.99	1
31 March–6 April 2019	Yes	Yes	RS	44.94	3
20 March–25 March 2020	Yes	Yes	Af	8.17	22
27 March–1 April 2020	Yes	Yes	RS	9.84	18
11 April–18 April 2020	Yes	Yes	RS	29.92	5

implies an enhanced possibility of non-AR IVT features being classified as ARs, we further checked to see if AR activities existed over any area in Iran for at least 24 h, thereby ensuring that an event satisfies the requirements of an "AR-1", the weakest category for an AR from the scale introduced by Ralph et al. (2019).

Over the study period, it was observed that AR conditions existed

during every year's most extreme events, along with the two extra extreme events in 2019 and 2020. Among them, only three years (2010, 2011, and 2013) had AR conditions for less than 24 h, with the shortest (2011) that lasted for 9 h. Furthermore, some events, such as the extreme rainfall event of 2004, could be traced back to multiple AR events affecting different regions of Iran.

Dezfuli (2019) observed that the sources of moisture for ARs that impact Iran come from the surrounding bodies of water, including the Mediterranean Sea, the Caspian Sea, the Persian Gulf, the Red Sea, and the Atlantic Ocean. From our analysis, we identify that the sources of moisture for ARs in the region are from the Atlantic Ocean via a northern Africa pathway and from the Red Sea via the Red Sea Strait (Bab-el-Mandeb). These pathways are also recognized in Esfandiari and Lashkari (2020). In Fig. 7, we showcase the three most observed AR lifecycles in the region: 1) those that propagate from the Atlantic Ocean over northern Africa without significant influence from the Red Sea (Fig. 7c, d) driven by the Saharan anticyclone (Shay-El et al., 1999), 2) those with moisture chiefly coming from the Red Sea (Fig. 7b) via the Red Sea Strait driven by a moisture transport at the 850 hPa level following a favorable position of the Arabian cyclone and mid-tropospheric troughs (Raziei et al., 2012) and 3) those which are created by merging bodies of moisture from both the Red Sea and the Atlantic Ocean (Fig. 7a, e), though the timing between ARs can vary between being simultaneous (Red Sea and African moisture at the same time; 2003 and 2019) and being subsequent (one source of moisture followed by other). Of these two different timings, it is the former that produces the events of greater volume, with the precipitation events of 2003 and 2019 being 4th and 1st heaviest by rainfall volume.

Table 1 showcases each AR with its pathway, determined by examining IVT objects at the 200 and 250 kg m⁻¹ s⁻¹ levels. Of the AR examined, three were found to come from moisture via the African pathway, seven from the Red Sea Strait, ten from both sources, and two from other sources (Gulf of Aden and Arabian Sea). This means that out of the 22 observed ARs, 17 were reliant on moisture fluxes from the Gulf of Aden while 13 could be linked to moisture transport over the African continent. Furthermore, each AR was ranked by the amount of precipitation it produced over Iran as calculated by CONNECT. The three highest ranking ARs all come from the three different AR classes, each occurring within the 2018–2019 period. Afterwards, ARs with moisture from both sources make up 7 out of 10 of the ARs ranked 4th to 13th, yet only 3 out of 9 of the ARs ranked 14th onwards are from both sources. In summary, ARs with moisture from both the African and Red Sea sources are the most frequently observed ARs that coincide with heavy precipitation over Iran.

Fig. 8 shows the accumulated amount of precipitation occurring during the events shown in Fig. 7. The most extreme event that occurred in Farvardin 2003, which was ranked the 4th greatest event by volume and propagated from the Red Sea and the Atlantic Ocean, mainly occurred in northeastern Iran. On the other hand, the heavy precipitation that occurred in Farvardin 2019 that involved the most extreme events in terms of volume during the last two decades and had similar pathway to that from 2003 mainly occurred over Southwestern Iran. This figure shows precipitation from the most extreme events in 2003, 2012, 2017, 2018, and 2019 and highlights that extreme events in recent Farvardins (2018 and 2019) are heavier than those of the past.

5. Conclusion

Spring precipitation, especially during the month of Farvardin, is important for Iranian agriculture. Over the past few years, an increase in the number of floods occurring after unprecedented rainfall events during the month of Farvardin have affected millions of people across Iran, caused the loss of life, damaged infrastructure, and engendered substantial economic losses in Iran's agriculture sector. The apparent increase in the number of floods during the last three years (2018–2020) led us to investigate the variations in different aspects of heavy

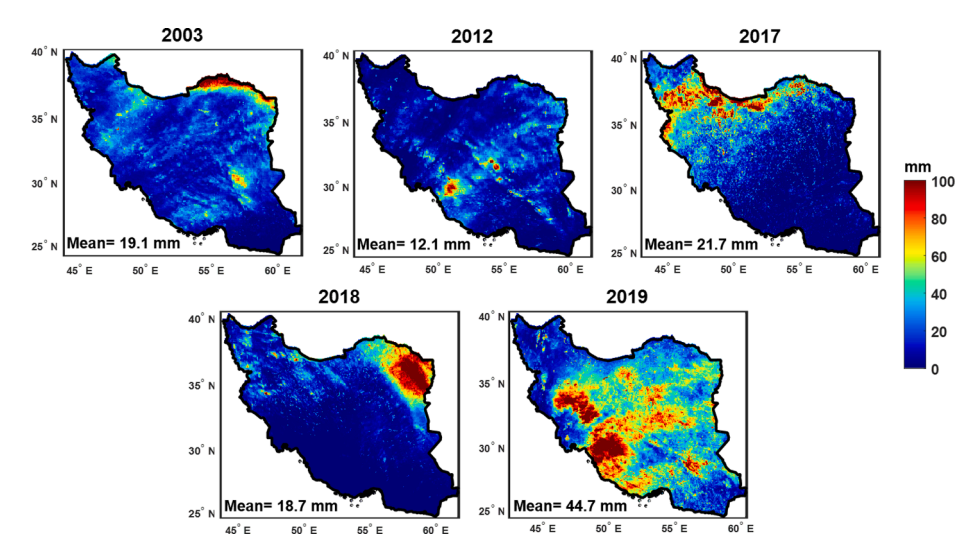


Fig. 8. PERSIANN-CCS estimates correspond to the heavy precipitation events shown in Fig. 7.

precipitation events like intensity and frequency, as well as their associated mechanisms during the month of Farvardin. To our knowledge, there is no study which explores the precipitation variations and mechanisms during this month.

The previous studies over Iran mainly focused on analyzing heavy precipitation at daily scales over the whole year. However, there is a need to assess the flood-causing short-duration heavy precipitation that occurs in early spring. In addition, using a limited number of synoptic gauge observations has hindered the ability to explore the variations in precipitation at a high spatial resolution. In this study, we applied the CONNECT algorithm with a 3 mm/3-hour threshold on the PERSIANN-CCS estimates at 0.04° spatial resolution to explore the variations in frequency, intensity, duration, and volume of heavy precipitation during Farvardin for the period from 2003 to 2020. The results indicated that increases in intensity and volume of heavy precipitation are the main reasons for the rising number of floods during Farvardin over the years 2018–2020. However, a significant increase in frequency and duration of heavy precipitation are not observed. The results also show that the frequency, intensity, duration, and volume of heavy precipitation was the highest in 2019 during the last two decades based on the PERSIANN-CCS estimates. This is also supported by the International Emergency Events database (https://www.emdat.be/) which ranked the floods in Farvardin 2019 as the costliest economic loss in Iranian history during the last two decades. Spatial analyses revealed that heavy precipitation events occurred over almost the entire country in Farvardin during the period 2003-2020 with the heaviest volume of rainfall hitting southwestern Iran in 2019 and the second highest volume in northeastern Iran in 2018. In addition, we observe that the spatiotemporal distribution of heavy precipitation events extracted by the CONNECT algorithm are consistent with extreme events occurred over Iran.

Investigating the presence of AR conditions on heavy precipitation events that occurred during the month of Farvardin revealed that ARs exist during every year's most extreme events. In addition, we classify the AR pathways that occurred in the country during Farvardin into three main categories. 1) ARs that propagated from the Atlantic Ocean via North Africa driven by the Saharan anticyclone, 2) ARs that propagated from the Red Sea via the Red Sea Strait and are influenced by the Arabian cyclone and mid-tropospheric troughs, 3) ARs created by merging bodies of moisture from both the Atlantic Ocean and the Red Sea. Our further investigations revealed that 8 out of 13 of the largest ARs over Iran come from moisture plumes with pathways over the African continent and the Red Sea.

Although this study mainly explored the variations of short-term precipitation over Iran for a specific month, the same procedure can

be followed for other regions. This study highlighted that the high spatial (0.04°) and temporal (3-hourly) resolution of PERSIANN-CCS at a global scale is an attractive feature for analyzing precipitation variations, especially over the countries with limited rain gauge observations. In addition, the CONNECT algorithm, which is an object-oriented tracking algorithm, can be used for the investigation of natural hazards associated with AR events such as floods and mudslides over different regions.

CRediT authorship contribution statement

Mojtaba Sadeghi: Conceptualization, Methodology, Software, Validation, Writing - original draft. Eric J. Shearer: Data curation, Methodology, Writing - review & editing. Hamidreza Mosaffa: Visualization, Investigation. Vesta Afzali Gorooh: Investigation. Matin Rahnamay Naeini: Visualization, Investigation. Negin Hayatbini: Investigation. Pari-Sima Katiraie-Boroujerdy: Investigation, Supervision. Bita Analui: Investigation, Supervision. Phu Nguyen: Methodology, Supervision. Soroosh Sorooshian: Methodology, Supervision.

Declaration of Competing Interest

The authors declare that they have no known competing financial interests or personal relationships that could have appeared to influence the work reported in this paper.

Acknowledgment

The financial support of this research is from the U.S. Department of Energy (DOE Prime Award DE-IA0000018), the California Energy Commission (CEC Award 300-15-005), University of California (4600010378 TO15 Am 22), Maseeh Fellowship, NOAA/NESDIS/NCDC (Prime Award NA09NES4400006 and NCSU CICS and Subaward 2009-1380-01), and the National Oceanic and Atmospheric Administration (#ST133017CQ0058) with Riverside Technology, Inc. We gratefully acknowledge the support of NVIDIA Corporation with the donation of the Quadra P6000GPU used for this research. Also, support from the office of the Vice-Chancellor for Research for Graduate Students, University of California, Irvine is acknowledged.

References

Alijani, B., 2002. Variations of 500 hPa flow patterns over Iranand surrounding areas and their relationship with the climate of Iran. Theor. Appl. Climatol. 72 (1-2), 41–54.

- Alijani, B., Harman, J.R., 1985. Synoptic climatology of precipitation in Iran. Ann. Assoc. Am. Geogr. 75 (3), 404–416.
- Alijanian, M., Rakhshandehroo, G.R., Mishra, A.K., Dehghani, M., 2017. Evaluation of satellite rainfall climatology using CMORPH, PERSIANN-CDR, PERSIANN, TRMM, MSWEP over Iran. Int. J. Climatol. 37 (14), 4896–4914.
- Aminyavari, S., Saghafian, B., Sharifi, E., 2019. Assessment of Precipitation Estimation from the NWP Models and Satellite Products for the Spring 2019 Severe Floods in Iran. Remote Sens. 11 (23), 2741.
- Asanjan, A. A., Faridzad, M., Hayatbini, N., Gorooh, V. A., Sadeghi, M., Shearer, E. J., Sorooshian, S., Nguyen, P., Hsu, K., & Taghian, M. (2019). An assessment of the unprecedented extreme precipitation events over Iran: From satellite perspective. Online at http://chrs.Web.Uci.Edu/Articles/Iran_rainfall.pdf.
- Ashouri, H., Hsu, K., Sorooshian, S., Braithwaite, D.K., Knapp., K.R., Cecil., L.D., Nelson, B.R., Prat, O.P., 2015. PERSIANN-CDR: Daily precipitation climate data record from multisatellite observations for hydrological and climate studies. Bull. Am. Meteorol. Soc.
- Azizi, G., Arsalani, M., Bräuning, A., Moghimi, E., 2013. Precipitation variations in the central Zagros Mountains (Iran) since A.D 1840 based on oak tree rings. Palaeogeogr., Palaeoclimatol., Palaeoecol. 386 (February 2019), 96–103. https:// doi.org/10.1016/j.palaeo.2013.05.009.
- Beck, H.E., Pan, M., Roy, T., Weedon, G.P., Pappenberger, F., van Dijk, A.I.J.M., Huffman, G.J., Adler, R.F., Wood, E.F., 2019. Daily evaluation of 26 precipitation datasets using Stage-IV gauge-radar data for the CONUS. Hydrol. Earth Syst. Sci. 23 (1), 207–224.
- Bitew, M.M., Gebremichael, M., 2010. Evaluation through independent measurements: Complex terrain and humid tropical region in Ethiopia. In: Satellite Rainfall Applications for Surface Hydrology. Springer, pp. 205–214.
- Boroujerdy, P.K., 2008. The analysis of precipitation variation and quantiles in Iran. In:
 Proceedings of the 3rd WSEAS International Conference on Energy & Environment.
 University of Cambridge, UK, pp. 248–253.
- Bozorgmehr, S., 2019. Iran says recent floods caused up to \$2.5 billion in damage. https://www.reuters.com/article/>.
- Conti, F. Lo., Hsu, K.-L., Noto, L.V., Sorooshian, S., 2014. Evaluation and comparison of satellite precipitation estimates with reference to a local area in the Mediterranean Sea. Atmos. Res. 138, 189–204.
- Darand, M., Daneshvar, M.R.M., 2014. Regionalization of precipitation regimes in Iran using principal component analysis and hierarchical clustering analysis. Environ. Process. 1 (4), 517–532.
- Davolio, S., Della Fera, S., Laviola, S., Miglietta, M.M., Levizzani, V., 2020. Heavy precipitation over Italy from the Mediterranean storm "Vaia" in October 2018: assessing the role of an atmospheric river. Mon. Weather Rev. 148 (9), 3571–3588.
- Dezfuli, A., 2019. Rare atmospheric river caused record floods across the Middle East. Bull. Am. Meteorol. Soc.
- Esfandiari, N., Lashkari, H., 2020. Identifying atmospheric river events and their paths into Iran. Theor. Appl. Climatol. 140 (3-4), 1125–1137.
- Feizi, V., Mollashahi, M., Farajzadeh, M., Azizi, G., 2014. Spatial and temporal trend analysis of temperature and precipitation in Iran. Ecopersia 2 (4), 727–742.
- Gelaro, R., McCarty, W., Suárez, M.J., Todling, R., Molod, A., Takacs, L., Randles, C.A., Darmenov, A., Bosilovich, M.G., Reichle, R., Wargan, K., Coy, L., Cullather, R., Draper, C., Akella, S., Buchard, V., Conaty, A., da Silva, A.M., Gu, W., Kim, G.-K., Koster, R., Lucchesi, R., Merkova, D., Nielsen, J.E., Partyka, G., Pawson, S., Putman, W., Rienecker, M., Schubert, S.D., Sienkiewicz, M., Zhao, B., 2017. The modern-era retrospective analysis for research and applications, version 2 (MERRA-2). J. Clim. 30 (14), 5419–5454.
- Guan, B., Waliser, D.E., 2015. Detection of atmospheric rivers: evaluation and application of an algorithm for global studies. J. Geophys. Res.: Atmos. 120 (24), 12514–12535.
- Hirpa, F.A., Gebremichael, M., Hopson, T., 2010. Evaluation of high-resolution satellite precipitation products over very complex terrain in Ethiopia. J. Appl. Meteorol. Climatol. 49 (5), 1044–1051.
- Hong, Y., Gochis, D., Cheng, J., Hsu, K., Sorooshian, S., 2007. Evaluation of PERSIANN-CCS rainfall measurement using the NAME event rain gauge network. J. Hydrometeorol. 8 (3), 469–482.
- Hong, Y., Hsu, K.-L., Sorooshian, S., Gao, X., 2004. Precipitation estimation from remotely sensed imagery using an artificial neural network cloud classification system. J. Appl. Meteorol. 43 (12), 1834–1853.
- Hsu, K.-L., Gao, X., Sorooshian, S., Gupta, H.V., 1997. Precipitation estimation from remotely sensed information using artificial neural networks. J. Appl. Meteorol. 36 (9), 1176–1190.
- Javari, M., 2016. Trend and homogeneity analysis of precipitation in Iran. Climate 4 (3), 44.
- Katiraie-Boroujerdy, P.-S., Rahnamay Naeini, M., Akbari Asanjan, A., Chavoshian, A., Hsu, K., Sorooshian, S., 2020. Bias correction of satellite-based precipitation estimations using quantile mapping approach in different climate regions of Iran. Remote Sens. 12 (13), 2102.
- Kousari, M.R., Ekhtesasi, M.R., Tazeh, M., Saremi Naeini, M.A., Asadi Zarch, M.A., 2011. An investigation of the Iranian climatic changes by considering the precipitation, temperature, and relative humidity parameters. Theor. Appl. Climatol. 103 (3-4), 321–335.
- Maggioni, V., Meyers, P.C., Robinson, M.D., 2016. A review of merged high-resolution satellite precipitation product accuracy during the Tropical Rainfall Measuring Mission (TRMM) era. J. Hydrometeorol. 17 (4), 1101–1117.
- Mahbod, M., Veronesi, F., Shirvani, A., 2019. An evaluative study of TRMM precipitation estimates over multi-day scales in a semi-arid region, Iran. Int. J. Remote Sens. 40 (11), 4143–4174.

- Moazami, S., Golian, S., Kavianpour, M.R., Hong, Y., 2013. Comparison of PERSIANN and V7 TRMM Multi-satellite Precipitation Analysis (TMPA) products with rain gauge data over Iran. Int. J. Remote Sens. 34 (22), 8156–8171.
- Modarres, R., da Silva, V. de P.R., 2007. Rainfall trends in arid and semi-arid regions of Iran. J. Arid Environ. 70 (2), 344–355.
- Mosaffa, H., Sadeghi, M., Hayatbini, N., Gorooh, V.A., Asanjan, A.A., Nguyen, P., Sorooshian, S., 2020a. Spatiotemporal variations of precipitation over Iran using the high-resolution and nearly four decades satellite-based PERSIANN-CDR dataset. Remote Sens. 12 (10), 1–14. https://doi.org/10.3390/rs12101584.
- Mosaffa, H., Shirvani, A., Khalili, D., Nguyen, P., 2020. Post and near real-time satellite precipitation products skill over Karkheh River Basin in Iran ABSTRACT. August 2019
- Mosaffa, H., Shirvani, A., Khalili, D., Nguyen, P., Sorooshian, S., 2020c. Post and near real-time satellite precipitation products skill over Karkheh River Basin in Iran. Int. J. Remote Sens. 41 (17), 6484–6502.
- Najafi, M.R., Moazami, S., 2016. Trends in total precipitation and magnitude–frequency of extreme precipitation in Iran, 1969–2009. Int. J. Climatol. 36 (4), 1863–1872.
- Nazaripour, H., Daneshvar, M.R.M., 2014. Spatial contribution of one-day precipitations variability to rainy days and rainfall amounts in Iran. Int. J. Environ. Sci. Technol. 11 (6), 1751–1758.
- Nazemosadat, M.J., Ghasemi, A.R., 2004. Quantifying the ENSO-related shifts in the intensity and probability of drought and wet periods in Iran. J. Clim. 17 (20), 4005–4018.
- Nguyen, P., Shearer, E.J., Tran, H., Ombadi, M., Hayatbini, N., Palacios, T., Huynh, P., Braithwaite, D., Updegraff, G., Hsu, K., 2019. The CHRS Data Portal, an easily accessible public repository for PERSIANN global satellite precipitation data. Sci. Data 6 (1). https://doi.org/10.1038/sdata.2018.296.
- Ralph, F.M., Rutz, J.J., Cordeira, J.M., Dettinger, M., Anderson, M., Reynolds, D., Schick, L.J., Smallcomb, C., 2019. A scale to characterize the strength and impacts of atmospheric rivers. Bull. Am. Meteorol. Soc. 100 (2), 269–289.
- Raziei, T., Daryabari, J., Bordi, I., Pereira, L.S., 2014. Spatial patterns and temporal trends of precipitation in Iran. Theor. Appl. Climatol. 115 (3-4), 531–540.
- Raziei, T., Mofidi, A., Santos, J.A., Bordi, I., 2012. Spatial patterns and regimes of daily precipitation in Iran in relation to large-scale atmospheric circulation. Int. J. Climatol. 32 (8), 1226–1237.
- Romilly, T.G., Gebremichael, M., 2011. Evaluation of satellite rainfall estimates over Ethiopian river basins. Hydrol. Earth Syst. Sci. 15 (5), 1505–1514.
- Rutz, J.J., Steenburgh, W.J., Ralph, F.M., 2014. Climatological characteristics of atmospheric rivers and their inland penetration over the western United States. Mon. Weather Rev. 142 (2), 905–921.
- Sadeghi, M., 2018. Assessment of the PERSIANN-CDR Products Bias-corrected with the GPCP Datasets Versions 2.2 & 2.3. UC Irvine.
- Sadeghi, M., Akbari Asanjan, A., Faridzad, M., Afzali Gorooh, V., Nguyen, P., Hsu, K., Sorooshian, S., Braithwaite, D., 2019a. Evaluation of PERSIANN-CDR constructed using GPCP V2. 2 and V2. 3 and a comparison with TRMM 3B42 V7 and CPC unified gauge-based analysis in global scale. Remote Sens. 11 (23), 2755.
- Sadeghi, M., Asanjan, A.A., Faridzad, M., Nguyen, P., Hsu, K., Sorooshian, S., Braithwaite, D., 2019b. PERSIANN-CNN: precipitation estimation from remotely sensed information using artificial neural networks-convolutional neural networks. J. Hydrometeorol. 20 (12), 2273–2289.
- Sadeghi, M., Nguyen, P., Hsu, K., Sorooshian, S., 2020. Improving near real-time precipitation estimation using a U-Net convolutional neural network and geographical information. Environ. Modell. Software 134, 104856. https://doi.org/ 10.1016/i.envsoft.2020.104856.
- Sadeghi, M., Nguyen, P., Rahnamay Naeini, M., Hsu, K., Braithwaite, D., Sorooshian, S., 2021. PERSIANN-CCS-CDR, a 3-hourly 0.04° global precipitation climate data record for heavy precipitation studies. Sci. Data. https://doi.org/10.1038/s41597-021-00940-9
- Saghafian, B., Haghnegahdar, A., Dehghani, M., 2017. Effect of ENSO on annual maximum floods and volume over threshold in the southwestern region of Iran. Hydrol. Sci. J. 62 (7), 1039–1049.
- Salmani-Dehaghi, N., Samani, N., 2019. Spatiotemporal assessment of the PERSIANN family of satellite precipitation data over Fars Province, Iran. Theor. Appl. Climatol. 138 (3-4), 1333–1357.
- Shay-El, Y., Alpert, P., da Silva, A., 1999. Reassessment of the moisture source over the Sahara Desert based on NASA reanalysis. J. Geophys. Res.: Atmos. 104 (D2), 2015–2030.
- Shearer, E.J., Nguyen, P., Sellars, S.L., Analui, B., Kawzenuk, B., Hsu, K., Sorooshian, S., 2020. Examination of global midlatitude atmospheric river lifecycles using an object-oriented methodology. J. Geophys. Res.: Atmos. 125 (22) e2020JD033425.
- Shearer, E.J., Phu, N., Afzali, V., Hsu, K., Sorooshian, S., 2021. Four Decades of Intensifying Precipitation from Tropical Cyclones. https://doi.org/10.21203/rs.3.rs-424061/v1.
- Shirvani, A., 2017. Change in annual precipitation in the northwest of I ran. Meteorol. Appl. 24 (2), 211–218.
- Soltani, S., Saboohi, R., Yaghmaei, L., 2012. Rainfall and rainy days trend in Iran. Clim. Change 110 (1-2), 187–213.
- Some'e, B.S., Ezani, A., Tabari, H., 2012. Spatiotemporal trends and change point of precipitation in Iran. Atmos. Res. 113, 1–12.
- Tabari, H., Somee, B.S., Zadeh, M.R., 2011. Testing for long-term trends in climatic variables in Iran. Atmos. Res. 100 (1), 132–140.
- Vaghefi, S.A., Keykhai, M., Jahanbakhshi, F., Sheikholeslami, J., Ahmadi, A., Yang, H., Abbaspour, K.C., 2019. The future of extreme climate in Iran. Sci. Rep. 9 (1), 1–11.
- Yadav, R.K., 2016. On the relationship between Iran surface temperature and northwest India summer monsoon rainfall. Int. J. Climatol. 36 (13), 4425–4438.

- Yang, D., Kane, D., Zhang, Z., Legates, D., Goodison, B., 2005. Bias corrections of long-term (1973–2004) daily precipitation data over the northern regions. Geophys. Res. Lett. 32 (19).
- Zarei, A.R., Masoudi, M., 2019. Trend assessment of climate changes in Iran. EQA-Int. J. Environ. Qual. 34, 1–16.
- Zarenistanak, M., Dhorde, A.G, Kripalani, R H, 2014. Trend analysis and change point detection of annual and seasonal precipitation and temperature series over southwest Iran. J. Earth Syst. Sci. 123 (2), 281–295.
- Zarrin, A., Ghaemi, H., Azadi, M., Farajzadeh, M., 2010. The spatial pattern of summertime subtropical anticyclones over Asia and Africa: a climatological review. Int. J. Climatol.: J. R. Meteorol. Soc. 30 (2), 159–173.